



# The sensitivity and specificity of $^{18}\text{F}$ -FDG PET/CT in spinal leptomeningeal metastases: the synergistic effect of the $^{18}\text{F}$ -FDG PET-CT to gadolinium-enhanced MRI

Zhe-Huang Luo<sup>1</sup>, Pu-Xuan Lu<sup>2</sup>, Wan-Ling Qi<sup>1</sup>, Ai-Fang Jin<sup>1</sup>, Qian Liu<sup>3</sup>, Qing-Yun Zeng<sup>1</sup>, Ping Lu<sup>1</sup>

<sup>1</sup>Department of Nuclear Medicine, Jiangxi Provincial People's Hospital, the First Affiliated Hospital of Nanchang Medical College, Nanchang, China; <sup>2</sup>Shenzhen Center for Chronic Disease Control, Shenzhen, China; <sup>3</sup>Department of Pathology, Jiangxi Provincial People's Hospital, the First Affiliated Hospital of Nanchang Medical College, Nanchang, China

**Contributions:** (I) Conception and design: ZH Luo; (II) Administrative support: ZH Luo, PX Lu; (III) Provision of study materials or patients: WL Qi, PX Lu, AF Jin, QY Zeng, P Lu; (IV) Collection and assembly of data: WL Qi, Q Liu, AF Jin, QY Zeng, P Lu; (V) Data analysis and interpretation: ZH Luo, WL Qi, PX Lu; (VI) Manuscript writing: All authors; (VII) Final approval of manuscript: All authors.

**Correspondence to:** Zhe-Huang Luo, MD. Department of Nuclear Medicine, Jiangxi Provincial People's Hospital, the First Affiliated Hospital of Nanchang Medical College, 152 Aiguo Rd., Donghu District, Nanchang 330006, China. Email: lzh6392@sina.com.

**Background:** Magnetic resonance imaging (MRI) plays an important role in the diagnosis of leptomeningeal metastases (LM); however, some sub-centimeter lesions may be missed. Positron emission tomography/computed tomography (PET/CT) has a high sensitivity and may play a synergistic role with MRI in diagnosing spinal LM (SLM). We aimed to retrospectively evaluate the detection of SLM with  $^{18}\text{F}$ -fluorodeoxyglucose PET/CT ( $^{18}\text{F}$ -FDG PET/CT) compared to that of whole spinal cord MRI in a single center.

**Methods:** Patients with SLM who had undergone  $^{18}\text{F}$ -FDG PET/CT and MRI were enrolled.  $^{18}\text{F}$ -FDG PET/CT imaging findings were independently reviewed by 2 nuclear medicine physicians.  $^{18}\text{F}$ -FDG PET/CT findings of SLMs were described. A consistency test was conducted to assess the patient-based diagnostic results obtained by the 2 physicians. Patient-based sensitivity, accuracy, and specificity in diagnosing SLM between  $^{18}\text{F}$ -FDG PET/CT and MRI of the whole spinal cord were compared using the chi-square or Fisher's exact test. A P value of  $<0.05$  was considered statistically significant. The receiver operating characteristic (ROC) curve was obtained to assess the diagnostic performance of maximum standardized uptake value (SUVmax) to diagnose SLM.

**Results:** A total of 16 patients with SLM were included in this study from October 2010 to April 2022. The primary tumor involved the lungs, liver, ovaries, prostate, esophagus, and unknown primary site. The mean age of patients, including 13 males and 3 females, was  $57.8 \pm 11.2$  (range, 34–73) years. Of 16 patients with SLM, 10 had nodular diseases, 2 had linear diseases, and 4 had mixed diseases. The kappa value of the consistency test of the 2 radiologists' diagnostic results was 0.765. The patient-based sensitivity, specificity, and accuracy of  $^{18}\text{F}$ -FDG PET/CT in diagnosing SLM were 87.5%, 89.2%, and 88.7%, respectively and those of whole spinal cord MRI were 75.0%, 100.0%, and 92.5%, respectively. There were no significant differences in sensitivity, specificity, and accuracy between the 2 methods, with P values of 0.654, 0.115, and 0.506, respectively. However, more nodular diseases were observed on PET/CT. The area under the ROC curve (AUC) for the prediction of SLM by SUVmax was 0.907 [95% confidence interval (CI): 0.831–0.983]. When  $\text{SUVmax} \geq 2.45$ , the Youden index was the largest, and the sensitivity and specificity were 89.3% and 75.7%, respectively.

**Conclusions:**  $^{18}\text{F}$ -FDG PET/CT is a good choice of imaging modality for assessing SLM. In the diagnosis of SLMs, PET/CT and enhanced MRI can play a better synergistic role.

**Keywords:** Leptomeningeal metastases (LM);  $^{18}\text{F}$ -fluorodeoxyglucose; positron emission tomography/computed tomography ( $^{18}\text{F}$ -FDG PET/CT); magnetic resonance imaging (MRI); diagnostic performance

Submitted Mar 08, 2023. Accepted for publication Sep 01, 2023. Published online Sep 22, 2023.

doi: 10.21037/qims-23-286

View this article at: <https://dx.doi.org/10.21037/qims-23-286>

## Introduction

Although central nervous system (CNS) metastases are not uncommon, they may occur in the brain, spinal cord, leptomeninges, epidural space, or dura (1). Leptomeningeal metastases (LMs) are rare, representing the 3<sup>rd</sup> common metastatic disorder of the CNS after brain metastases and epidural metastasis (2). Leptomeninges include the pia mater, arachnoid, and subarachnoid space. Patients with LM will develop neurological symptoms in a short period. Early detection, early diagnosis, and early intervention can help prolong the patient's survival time and maintain the quality of life; however, the patient's initial symptoms may be not specific (3). The diagnosis of LM usually depends on neurological symptoms, comprehensive neurological exam, enhanced magnetic resonance imaging (MRI), and cerebrospinal fluid (CSF) testing. MRI plays an important role in the diagnosis of LM (4), and sometimes the typical MRI enhancement findings combined with the history can make a correct diagnosis without cytology (3,4). However, the view field of MRI is limited and some early LMs are not easily observable on MRI.

$^{18}\text{F}$ -fluorodeoxyglucose ( $^{18}\text{F}$ -FDG) positron emission tomography/computed tomography (PET/CT) is a useful tool for staging and restaging malignant tumors (5). Compared with MRI, the advantage is that it is a whole-body examination, meaning that hypermetabolic metastases anywhere in the body, including LM, can be detected. Some case reports have reported that LM were FDG-avid (6-8). To date, the application of PET/CT in the spinal LM (SLM) has been reported (9-11). To investigate the role of  $^{18}\text{F}$ -FDG PET/CT in SLM, we retrospectively analyzed  $^{18}\text{F}$ -FDG PET/CT findings of SLM and evaluated the diagnostic performance of  $^{18}\text{F}$ -FDG PET/CT in SLM in this study. We present this article in accordance with the STARD reporting checklist (available at <https://qims.amegroups.com/article/view/10.21037/qims-23-286/rc>).

## Methods

### *Ethical approval*

The study was conducted in accordance with the Declaration of Helsinki (as revised in 2013). The study was approved by institutional Ethics Committee of Jiangxi Provincial People's Hospital and the requirement for individual consent for this retrospective analysis was waived.

### *Study population*

We retrospectively analyzed  $^{18}\text{F}$ -FDG PET/CT of patients with malignancy and suspected SLM. The inclusion criteria were as follows: (I)  $^{18}\text{F}$ -FDG PET/CT was performed consecutively in our hospital between October 2010 and April 2022; (II) there were documented histopathological diagnoses of primary cancers; (III) SLM was suspected because of neurological signs and symptoms; (IV) the patient had also undergone an MRI of the whole spinal cord within 1 month prior or post to PET/CT. The exclusion criteria were as follows: (I) invasion and compression of the spinal cord by adjacent bone tumors or only epidural metastasis; (II) only intramedullary metastases; (III) involvement of the spinal cord by lymphoma.

### *Diagnostic criteria for SLM*

SLM was diagnosed based on the European Association of Neuro-Oncology-European Society for Medical Oncology (EANO-ESMO) Clinical Practice Guidelines for diagnosis, treatment, and follow-up of patients with LM from solid tumors (12), which is the first European guide in this field.

### *$^{18}\text{F}$ -FDG PET/CT imaging and image analysis*

All patients were instructed to fast for at least 6 hours and to limit their physical exertion at least 24 hours before the

$^{18}\text{F}$ -FDG injection. Each patient, whose blood glucose level remained in a normal range (or less than 10 mmol/L in patients with diabetes), was injected via a venous line with an activity of mean 296 MBq (according to body weight, 5.5 MBq/kilogram)  $^{18}\text{F}$ -FDG. The patient was rested for a scheduled 45–60-minute uptake period followed by image acquisition on PET/CT scanner (Discovery STE; GE Healthcare, Chicago, IL, USA). The patient emptied their bladder regularly before the acquisition of images, and no oral or intravenous contrast was administered. Low-dose CT from the vertex of the skull to the upper thigh with the patient supine was performed for PET attenuation correction and anatomical location. PET data were acquired covering the same area in 3-dimensional (3D) mode, and the acquisition time per bed position was 2.5 or 3.0 minutes, with a total of 6–8 bed positions acquired. PET images were reconstructed with iterative methods after correction for scatter, dead time, random coincidences, and decay. The images were reformatted into axial data sets and were reviewed on a picture-archiving and communication system (PACS) workstation (GE AW 4.6 workstation; GE Healthcare) displaying a maximum-intensity projection (MIP) image and multiplanar PET, CT, and PET/CT fusion images and analyzed visually and semi-quantitatively with the measurement of the maximum standardized uptake value (SUV<sub>max</sub>). The SUV values were generated utilizing the patient's body mass index (BMI). The SUV of the lesions or spinal cord was measured by placing the cursor at the region of interest (ROI) and 1-click measurement of workstation AW4.6. SLM was observed through MIP images of  $^{18}\text{F}$ -FDG PET/CT scan, axial and sagittal CT, PET, and fusion PET/CT images of the entire spinal canal.

All images were reviewed independently by 2 board-certified nuclear medicine physicians with 5 and 10 years of experience in whole-body PET/CT analysis. They were aware of the cancer histories of patients but did not know if SLM were present. PET/CT images were analyzed visually as well as semiquantitatively, with measurement of SUV<sub>max</sub>. If SUV<sub>max</sub> >2.5, spinal leptomeningeal SUV<sub>max</sub> ≥ SUV<sub>liver</sub>, then SLM was considered. The diagnostic consistency was assessed. Any disagreement was settled through negotiation, with the negotiation results serving as the final diagnosis. Diagnostic performance was evaluated by comparing the diagnosis of  $^{18}\text{F}$ -FDG PET/CT and MRI.

### *Documented MRI report review*

Enhanced MRI is the preferred method if SLM is suspected.

Spinal leptomeningeal enhancement and nodular changes are the most common finding of SLMs. As the MRIs had predominantly been conducted from external hospitals, the documented MRI reports were reviewed.

### *Follow-ups*

All patients who were suspected of SLM were followed up by telephone, webchat, or clinic. The follow-up contents included clinical manifestations, routine or enhanced MRI of the whole spinal cord, and PET/CT examination if necessary. The follow-up period was 3 months to 2 years and ended on 31 April 2022.

### *Statistical analysis*

Data was analyzed in SPSS1 (IBM Corp., Armonk, NY, USA). We used descriptive analyses for demographics, tumor characteristics, and the FDG uptake semi-quantitative parameter SUV<sub>max</sub>. Consistency tests were conducted to evaluate diagnostic results between 2 physicians, with the following evaluation criteria of value: kappa value ≥0.75 represented that the diagnostic results were in good consistency; 0.4 ≤ kappa value <0.75 represented that the diagnostic results were in general consistency; kappa value <0.4 represented that the diagnostic results were in poor consistency. Patient-based sensitivity, accuracy, and specificity between  $^{18}\text{F}$ -FDG PET/CT and MRI were compared using the chi-square or Fisher's exact test. A P value of <0.05 was considered statistically significant. To assess the diagnostic performance of SUV<sub>max</sub> to diagnose SLM, receiver operating characteristic (ROC) curves were obtained, and the sensitivity and specificity based on the optimal cut-off value of SUV<sub>max</sub> were calculated.

## **Results**

### *Demographics and clinical characteristics of patients*

From October 2010 to April 2022, a total of 135 patients clinically suspicious of intraspinal metastases (IMs) underwent  $^{18}\text{F}$ -FDG PET/CT imaging. Of them, no IM was observed in 37 cases, radiation myelitis in 1 case, invasion or/and compression of the spinal cord by adjacent bone tumors (without SLM in other segments) in 60 cases, epidural metastasis only in 2 cases, spinal cord infiltration of lymphoma in 17 cases, intramedullary metastases only in 2 cases, and SLM in 16 cases (with or without epidural/intramedullary metastasis). A total of 16 patients were

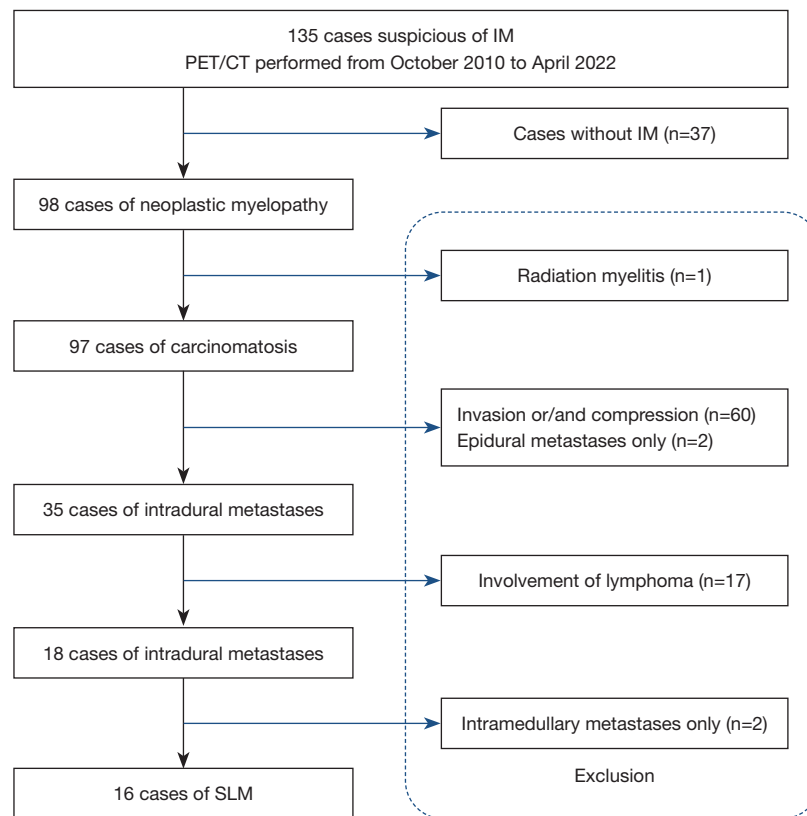


**Figure 1** Flow diagram of enrolled patients. IM, intraspinal metastasis; PET, positron emission tomography; CT, computed tomography; SLM, spinal leptomeningeal metastasis.

finally included in this study (*Figure 1*), and 37 patients without IMs were used as a control group.

The mean age of the 16 patients with SLM, including 13 males and 3 females, was  $57.8 \pm 11.2$  (range, 34–73) years. All 16 patients with SLM presented with neurological dysfunction of the lower extremities. The common manifestations were pain, sensory disturbances, weakness, walking instability, gait disturbance, and paraplegia. Sphincter disturbance was experienced by 4 patients. The primary tumor involved the lungs in 9 cases (56.3%, 8 squamous cell carcinomas and 1 adenocarcinoma), liver in 2 cases (12.5%, hepatocellular carcinoma), ovary in 1 case (6.3%, serous cystadenocarcinoma), prostate in 1 case (6.3%), pancreas in 1 case (6.3%), esophagus in 1 case (6.3%), and unknown primary site in 1 case (6.3%, biopsy showed metastasis in resected cervical lymph nodes). The mean time from diagnosis of the primary tumor to diagnosis of SLM was 9.3 (range, 1–26) months. The mean time between diagnosis of SLM and death was 7.4 (range, 1–15) months. SLM was found at diagnosis of the primary

tumor in 5 (31.3%) cases, and after treatment of the primary tumor in 11 (68.8%) cases. All patients (100.0%) were found to have metastasis to the other organs/tissue before or at the same time as SLM (*Table 1*), with lymph node involvement (12 cases, 75.0%) being most frequently observed, followed in order from most to least by bone (5 cases, 31.3%), brain parenchyma (4 cases, 25.0%), liver (3 cases, 18.8%), lung (2 cases, 12.5%), adrenal (2 cases, 12.5%), soft tissue (2 cases, 12.5%), and kidney (1 case, 6.3%).

The characteristics of the 37 patients without SLM were summarized in *Table S1*.

### *SLM locations and $^{18}\text{F}$ -FDG PET/CT findings*

In 16 patients with SLM, SLM affected the thoracic region in 13 cases (the most common site was at the T11–12 level), lumbar and sacral in 8 cases, and cervical in 3 cases. SLM was associated with epidural metastasis in 2 cases and intramedullary metastasis in 3 cases. On  $^{18}\text{F}$ -FDG PET/CT, SLM appeared as nodular disease in 10 cases, linear disease

**Table 1** Clinical data of 16 patients with SLM

No.	Sex	Age (years)	Primary tumor site	SLM at level	Intraspinal location			SUVmax	Brain/vertebrae metastasis	Other systemic metastasis
					ED	SLM	IMM			
1	M	48	Lung	L1		+	1.8	Brain (pri)	LNs	
2	M	38	Prostate*	T11–12		+	2.7	Vertebrae (sim)	OB	
3	M	34	Liver	T11–12		+	1.9		LNs, lung	
4	M	70	Esophagus	L1–2		+	5.6		Liver, LNs, adr	
5	M	61	Lung	T7		+	+	6.4		LNs
				T11		+	+	7.7		
6	M	60	Lung	T1		+		9.5	Vertebrae (pri)	LNs, Kid, OB
				T3		+		9.5		
				L2		+		2.9		
				L3		+		11.8		
				L5		+		4.2		
				S1	+			7.7		
7	M	67	Lung	T11		+		4.9	Vertebrae (pri)	OB
				L4		+		3.5		
8	F	63	Lung*	T12		+	4.8		LNs	
9	M	61	Lung	L3		+	13.9	Brain (pri)	LNs	
				T2–3		+	9.6			
10	M	44	Liver	T11–12		+	2.7	Vertebrae (pri)	Lung, OB	
				S1	+		3.3			
11	F	73	Ovary*	T12–L1		+	+	2.6	Vertebrae (sim)	Liver, LNs, ST
12	M	54	Pancreas	T12		+		4.4		Liver, LNs, ST, OB
13	M	62	Lung*	C4–5		+		6.3		LNs
14	F	65	Unknown	T12–L2		+		2.4	BLM (pri)	
15	M	60	Lung*	C7		+		3.2	Brain (pri)	adr, LNs
				T12		+		4.5		
				L1		+		2.5		
				L2		+		6.3		
				L3		+		4.8		
				L4		+		2.8		
16	M	64	Lung	L1		+		4.3	Brain	LNs

+, metastases found at different sites; \*, SLM found at diagnosis of primary cancer. SLM, spinal leptomeningeal metastasis; ED, epidural metastasis; IMM, intramedullary metastasis; SUVmax, maximum standardized uptake value; M, male; pri, detected prior to SLM; LN, lymph nodes; sim, detected simultaneously with SLM; OB, other bone(s); adr, adrenal; Kid, kidney; F, female; ST, soft tissue; BLM, brain leptomeningeal metastasis.

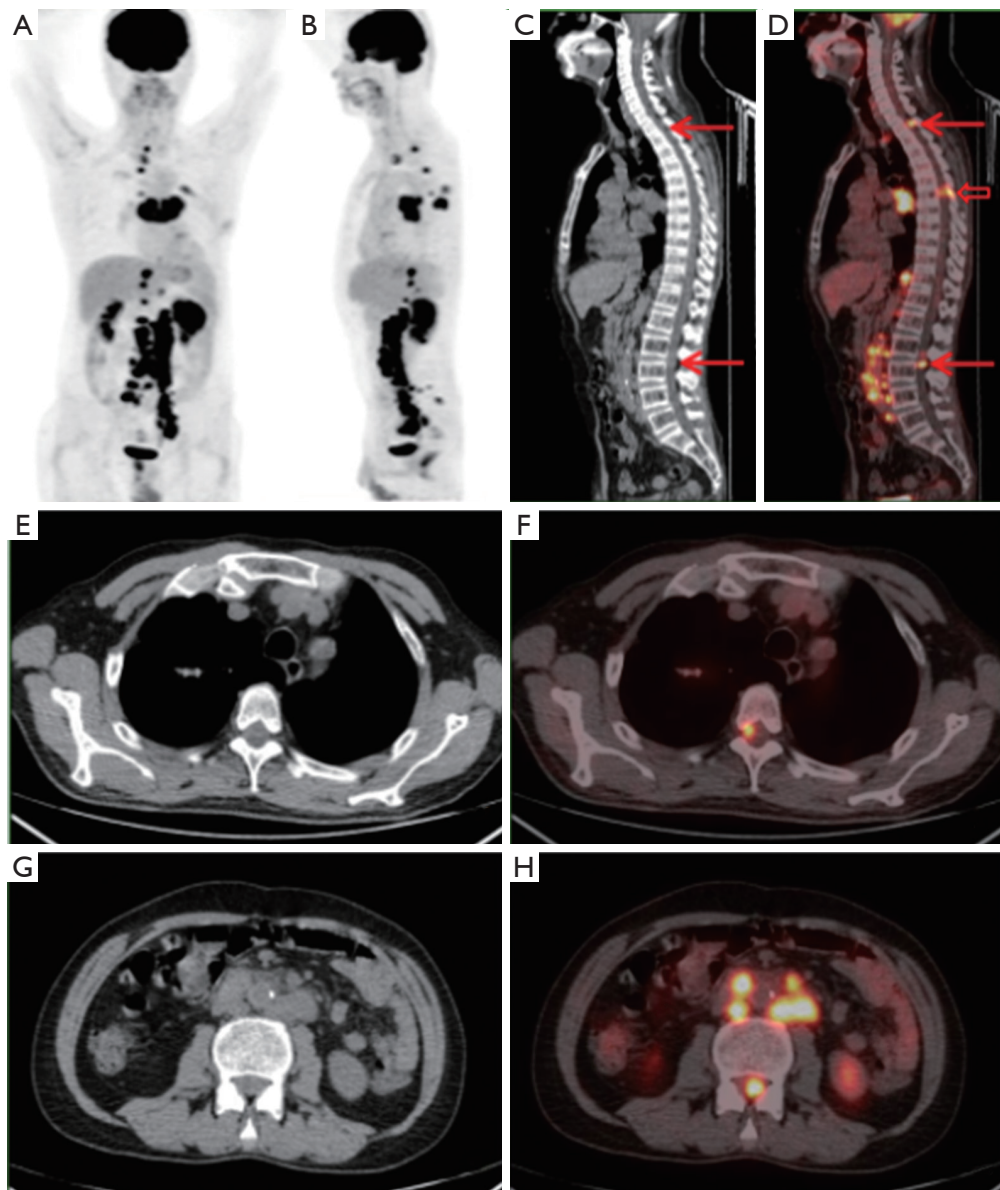


**Figure 2**  $^{18}\text{F}$ -FDG PET/CT of a 60-year-old male performed 17 months after surgery for lung adenocarcinoma. Multiple hypermetabolic lesions were revealed on anterior and lateral PET MIP views (A,B). Multiple nodular SLMs are distributed along the spinal cord (arrows; C,D: midline sagittal CT and fusion PET/CT images. Blank arrow: spinal metastasis). The SLMs push against the spinal cord (E,F: axial CT and fusion PET/CT images at T3 level) and cauda equina (G,H: axial CT and fusion PET/CT images at L3 level).  $^{18}\text{F}$ -FDG,  $^{18}\text{F}$ -fluorodeoxyglucose; PET, positron emission tomography; CT, computed tomography; MIP, maximum intensity projection; SLMs, spinal leptomeningeal metastases.

in 2 cases, and mixed diseases in 4 cases. In 10 patients with nodular disease, a total of 22 nodular lesions were observed, including single nodules (5 cases, 31.3%) and multiple nodules (5 cases, 31.3%); in 4 patients with mixed disease, 3 nodules (2 cases, 12.5%) were observed. The SUVmax of

SLM ranged from 1.8 to 13.9 [mean  $\pm$  standard deviation (SD):  $5.3 \pm 3.1$ ] (Figures 2-5).

Of 37 patients without SLM, 4 patients had linear uptake in the spinal leptomeninges, 2 in the neck segment, and 2 in the thoracolumbar segment.

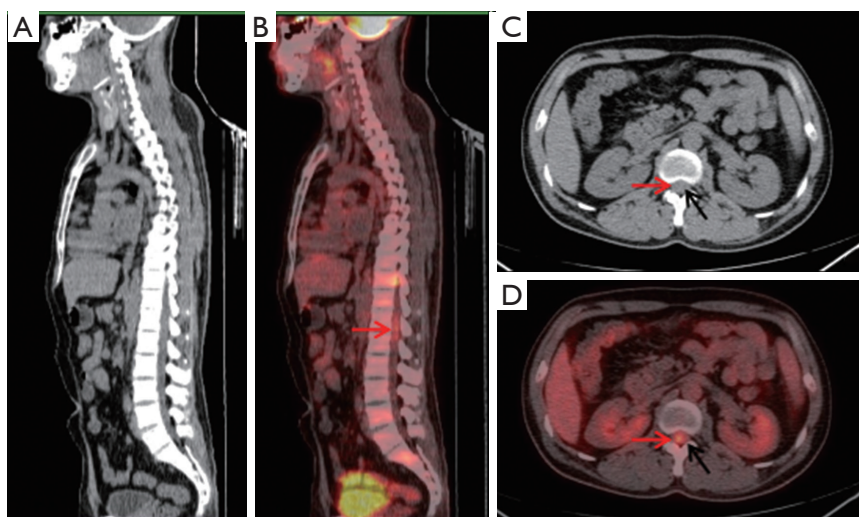


**Figure 3**  $^{18}\text{F}$ -FDG PET/CT of a 38-year-old male with prostate cancer. Patchy FDG-avid SLM at T11–12 level is revealed on fusion PET/CT images corresponding to segmental swelling spinal cord on sagittal CT (A,B). The SLM located on the side of the spine push against the spinal cord (C,D: axial CT and fusion PET/CT images at T12 level). Red arrows: SLM; black arrows: spinal cord.  $^{18}\text{F}$ -FDG,  $^{18}\text{F}$ -fluorodeoxyglucose; PET, positron emission tomography; CT, computed tomography; SLM, spinal leptomeningeal metastasis.

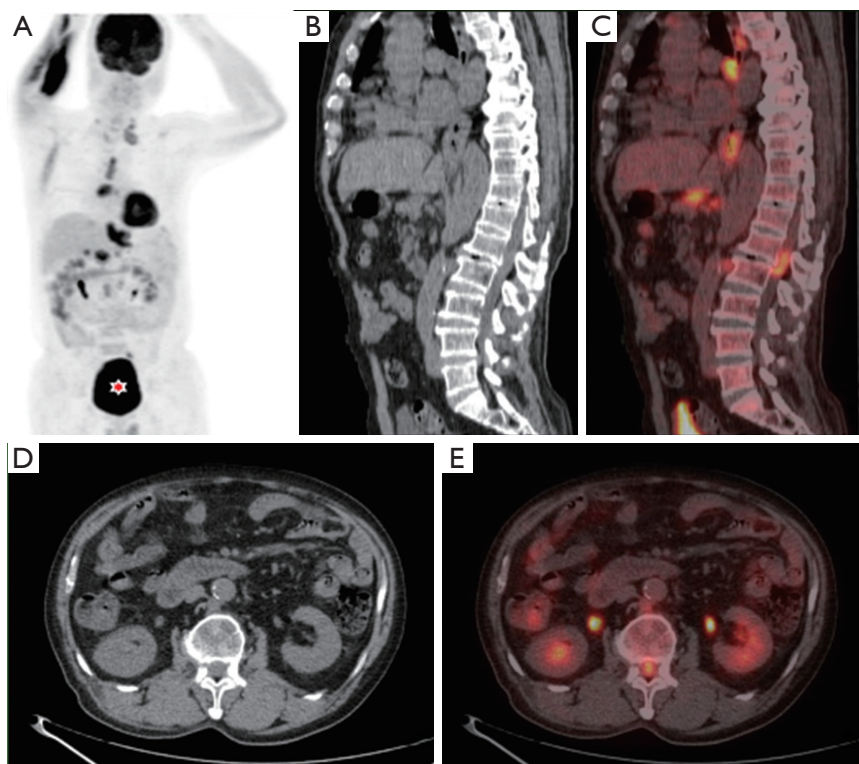


**Figure 4**  $^{18}\text{F}$ -FDG PET/CT of a 70-year-old male with esophageal cancer 8 months after radiotherapy. Multiple hypermetabolic lesions and urinary retention (star) are shown near the midline on PET MIP (A). Linear FDG-avid SLM at L1–2 level is revealed on sagittal fusion PET/CT images corresponding to segmental swelling cauda equina on sagittal CT (B,C). Swelling cauda equina with FDG avidity is shown on axial CT and fusion PET/CT images at the 12th thoracic level (D,E).  $^{18}\text{F}$ -FDG,  $^{18}\text{F}$ -fluorodeoxyglucose; PET, positron emission tomography; CT, computed tomography; MIP, maximum intensity projection; SLM, spinal leptomeningeal metastasis.

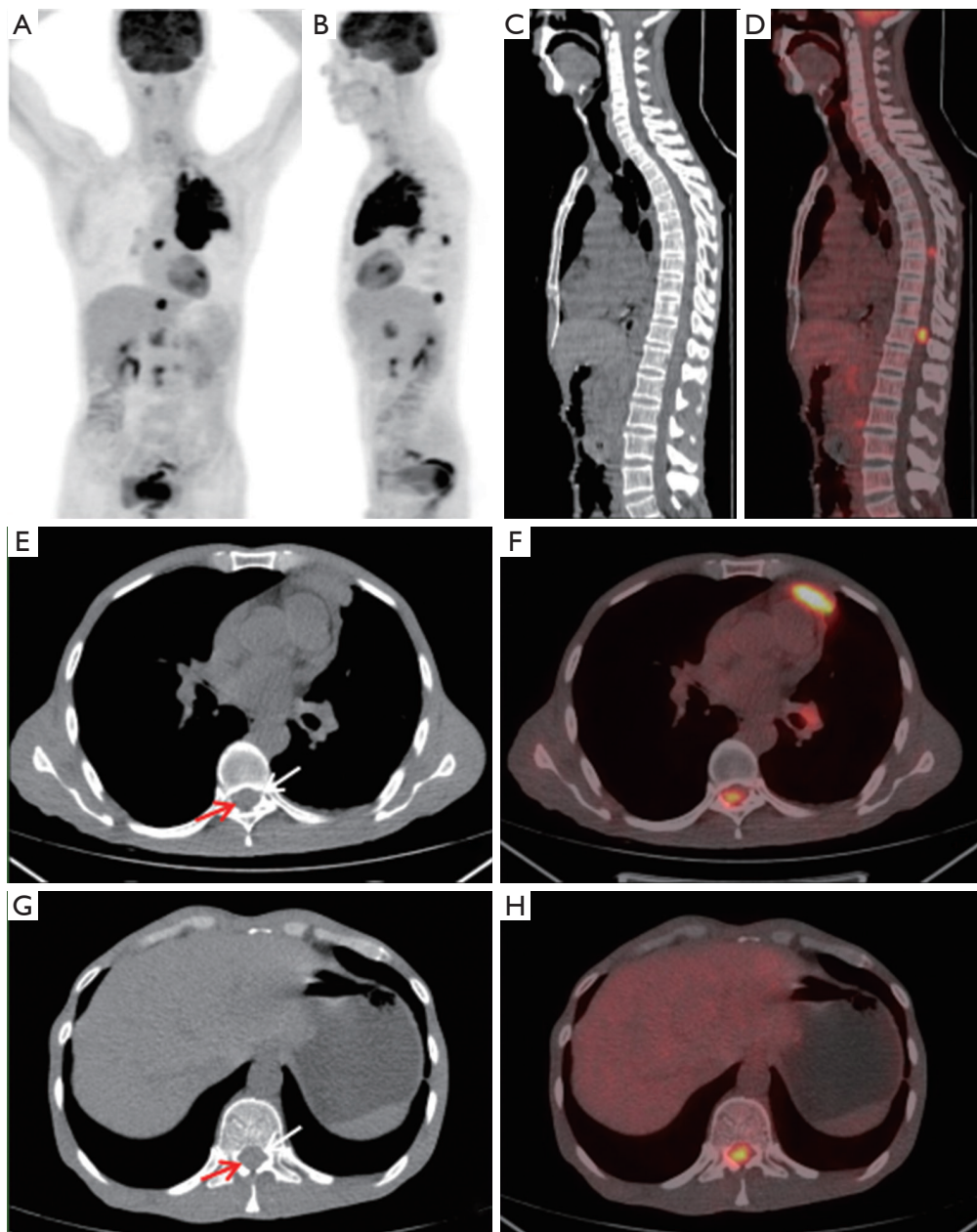


**Figure 5**  $^{18}\text{F}$ -FDG PET/CT of a 61-year-old male with lung adenocarcinoma. A hypermetabolic large mass in the lung and multiple nodules with FDG uptake near midline are revealed on anterior and lateral PET MIP views (A,B). Two SLMs are distributed along the spinal cord (C,D: midline sagittal CT and fusion PET/CT images). The SLMs (red arrows) push against the spinal cord (white arrows; E-H: axial CT, and fusion PET/CT images at T7 and T11 level).  $^{18}\text{F}$ -FDG,  $^{18}\text{F}$ -fluorodeoxyglucose; PET, positron emission tomography; CT, computed tomography; MIP, maximum intensity projection; SLMs, spinal leptomenigeal metastases.



### MRI and follow-ups of patients

All 16 patients with SLM had undergone whole spinal cord enhanced MRI within 2 weeks prior to (5 cases, 31.3%) or post (11 cases, 68.8%)  $^{18}\text{F}$ -FDG PET/CT. The CSF cytological study was performed in 8 (50%) cases. The types of SLM are shown in *Table 2*.

Of 37 cases without IM, 19 (51.4%) patients had undergone whole spinal cord enhanced MRI within 2 weeks prior to (4 cases, 10.8%) or post (7 cases, 18.9%) PET/CT, within 1 month post PET/CT (8 cases, 21.6%); the other 18 (48.6%) patients had undergone non-contrast MRI within 2 weeks prior to (7 cases, 18.9%) or post (5 cases, 13.5%) PET/CT, within 1 month post PET/CT (6 cases, 16.2%). MRI prior to and post PET/CT showed no abnormality in 4 patients with linear FDG uptake in the SLM, these 4 patients had not received treatment related to SLM.

**Table 2** Type of SLM in 16 patients\*

Type	Number	Confirmed/probable/possible
IA	2	Confirmed
IB	3	Confirmed
IC	1	Confirmed
ID	0	–
IIA	0	–
IIB	7	Probable
IIC	3	Probable
IID	0	–

\*, based on EANO-ESMO Clinical Practice Guidelines for diagnosis, treatment, and follow-up of patients with leptomeningeal metastasis from solid tumors. SLM, spinal leptomeningeal metastasis; EANO-ESMO, European Association of Neuro-Oncology-European Society for Medical Oncology.

**Table 3** Comparison of  $^{18}\text{F}$ -FDG PET/CT and MRI in diagnosis of SLM

Imaging modalities	Patients with SLM (n=16)		Patients without IM (n=37)		Sensitivity (%)	Specificity (%)	Accuracy (%)
	Positive	Negative	Negative	Positive			
PET/CT	14	2	33	4	87.5	89.2	88.7
MRI	12	4	37	0	75.0	100.0	92.5

The sensitivity, specificity and accuracy difference between PET/CT and MRI was not significant, P values were 0.654, 0.115, and 0.506, respectively.  $^{18}\text{F}$ -FDG,  $^{18}\text{F}$ -fluorodeoxyglucose; PET, positron emission tomography; CT, computed tomography; MRI, magnetic resonance imaging; SLM, spinal leptomeningeal metastasis; IM, intraspinal metastasis.

### Diagnostic performance of $^{18}\text{F}$ -FDG PET/CT and ROC curve analysis to determine the cut-off value of SUVmax

The patient-based  $^{18}\text{F}$ -FDG PET/CT diagnostic results between the 2 nuclear medicine physicians were in good consistency (kappa value =0.765).

On PET/CT, the diagnosis of SLM was missed in 2 out of 16 (12.5%) patients and 4 out of 37 (10.8%) patients without IM were misdiagnosed with SLM. The patient-based sensitivity, specificity, and accuracy of  $^{18}\text{F}$ -FDG PET/CT in diagnosing SLM were 87.5%, 89.2%, and 88.7%, respectively, and the patient-based sensitivity, specificity, and accuracy of MRI were 75.0%, 100.0%, and 92.5%, respectively. The sensitivity, specificity, and accuracy between  $^{18}\text{F}$ -FDG PET/CT and MRI had no significant difference, with P values of 0.654, 0.115, and 0.506, respectively (*Table 3*, *Tables S2,S3*). However, in a total of 25 nodular lesions showing in PET/CT, MRI showed only 16 nodular diseases; all nodules showed in MRI were observed on PET/CT. In 1 patient with linear SLM, PET/CT showed a larger range of linear disease than MRI (*Figure 6*).

The ROC curve of the total SUVmax of SLM in the 16 cases was plotted to compare with those in 37 non-SLM cases (4 of them had linear FDG uptake. The SUVmax in the other 33 patients represented the SUVmax of the whole spinal cord). The area under the ROC curve (AUC) for the prediction of SLM by SUVmax was 0.907 [95% confidence interval (CI): 0.831–0.983] (*Figure 7*). When SUVmax  $\geq 2.45$ , the Youden index was the largest, and the sensitivity and specificity were 89.3% and 75.7%, respectively.

### Discussion

SLM is generally considered an important complication of solid tumors (13). If not correctly recognized and promptly treated, it may lead to irreversible neurological deficit. In

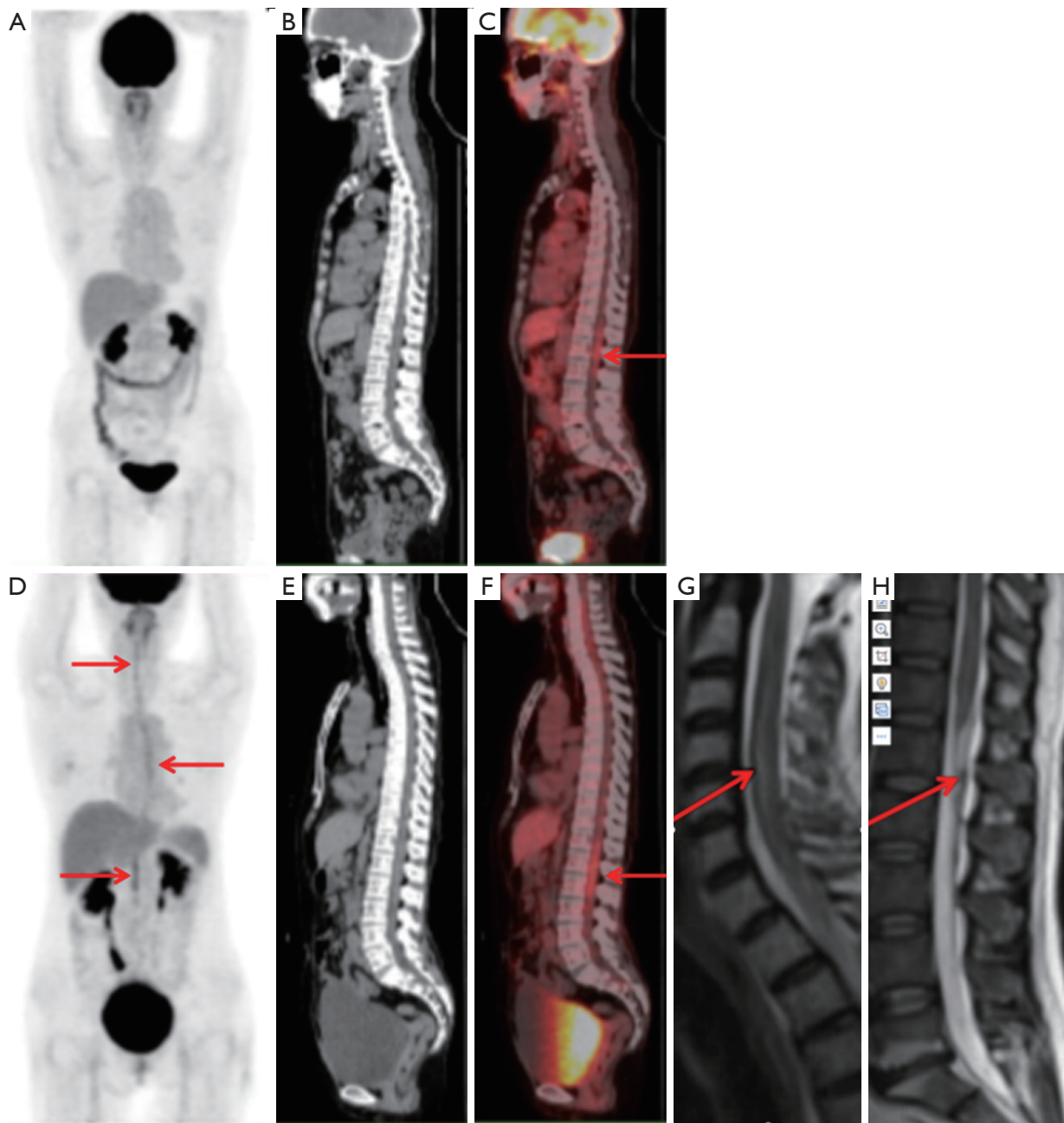


**Figure 6** Whole body  $^{18}\text{F}$ -FDG PET/CT and spinal MRI of a 65-year-old male with unknown primary malignancy. The lymph node resection in the left neck led to the diagnosis of lymph node metastasis. No primary lesion was observed, but SLMs was suspected on PET/CT (A-C). SLMs was confirmed by MRI and PET/CT review (and cytology of cerebrospinal fluid) 5 months later (D-H: note the bladder retention). (A,D) PET MIP map. (B,E) Midline sagittal CT. (C,F) Sagittal fusion images. (G,H) MRI T2W midline sagittal image. Red arrows: SLMs.  $^{18}\text{F}$ -FDG,  $^{18}\text{F}$ -fluorodeoxyglucose; PET, positron emission tomography; CT, computed tomography; MRI, magnetic resonance imaging; SLMs, spinal leptomeningeal metastases; MIP, maximum intensity projection; T2W, T2-weighted.

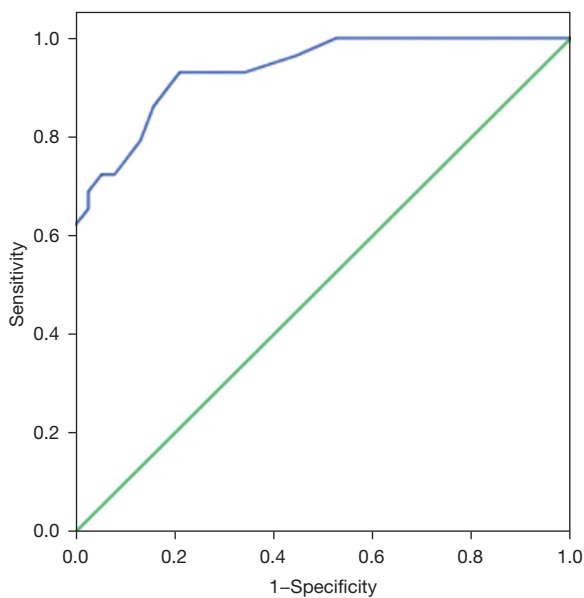


**Figure 7** Sensitivity and specificity of ROC curve in predicting SLMs by SUVmax. ROC, receiver operating characteristic; SLMs, spinal leptomeningeal metastases; SUVmax, maximum standardized uptake value.

this study, we evaluated the role of  $^{18}\text{F}$ -FDG PET/CT in the diagnosis of LM. To the best of our knowledge, no large series  $^{18}\text{F}$ -FDG PET/CT study on SLM has been published in English literature.

LM is a devastating condition; the prognosis of patients with LM remains dismal, the majority of patients expire within several weeks or months of diagnosis, regardless of the strategy of therapy (4). A study found that 19% of patients with solid tumors had undiagnosed or asymptomatic LM in an autopsy series (14). The incidence of LM seems to be increasing due to improved diagnostic sensitivity and the increased survival span of cancer patients (3).

Previous case reports (6-9) have shown that SLM exhibits nodular or linear FDG uptake on  $^{18}\text{F}$ -FDG PET/CT, which was also demonstrated by our study. SLM may be a single or multiple lesion. These findings are non-specific, and other disorders have similar findings (15-17), such as primary tumors with nodular FDG uptake and longitudinal myelitis with linear FDG uptake. However, combined with the patient's malignancy history, the diagnostic performance of PET/CT is greatly improved. In our group, the patient-based sensitivity, specificity, and accuracy of  $^{18}\text{F}$ -FDG PET/CT in diagnosing SLM were 87.5%, 89.2%, and 88.7%, respectively.

Gadolinium-enhanced MRI of the whole spinal cord is the current imaging modality for the diagnosis of SLM (13,18), it shows the location and extent of SLM. The sensitivity of gadolinium-enhanced MRI is about 70%, with specificity of 77–100%. In this study,  $^{18}\text{F}$ -FDG PET/CT has a similar effect. Compared with MRI, we found that there was no significant difference in patient-based sensitivity, specificity, and accuracy of SLM diagnosis.  $^{18}\text{F}$ -FDG PET/CT revealed earlier metastasis, including some subcentimeter lesions. However, it inevitably led to some false positives, which related to the physiological FDG uptake of the normal spinal cord. There were almost no false positives in MRI in our study. Further, the view field of MRI is limited, but PET/CT is a whole-body exam, which can be used for comprehensive evaluation of cancer patients besides intraspinal lesions. SLM is usually end metastasis, it is often accompanied by metastasis to other tissues or organs. MRI lacks the advantage of this systemic assessment, which is important for the therapy regimen of cancer patients. In our cases, all patients had metastasis to other tissues or organs. SLM can be disseminated by CSF. Of these 16 SLM patients,  $^{18}\text{F}$ -FDG PET/CT revealed that 10 had metastases to the brain or vertebrae. Despite the improved diagnostic capability,  $^{18}\text{F}$ -FDG PET images sometimes may not accurately distinguish intramedullary metastases from epidural tumors due to limitations in image resolution. Contrast-enhanced MRI may help with location and confirmation. The diagnostic role of  $^{18}\text{F}$ -FDG PET-CT and enhanced MRI is complementary, as opposed to one imaging modality being superior to the other (19).

It is worth noting that partial spinal segments show physiological relatively increased uptake of  $^{18}\text{F}$ -FDG (Figure S1), typically peaking at the level of the 4<sup>th</sup> cervical vertebra and the 11<sup>th</sup> to 12<sup>th</sup> thoracic vertebra (20,21). Its intensity was almost 30% higher than the hepatic FDG intensity, according to both visual and semi-quantitative assessment (SUV value). Nuclear physicians should be aware of this possible diagnostic pitfall. To assess the diagnostic performance of  $^{18}\text{F}$ -FDG PET/CT, ROC analysis was performed by evaluating the semiquantitative parameter SUVmax in differentiating equivocal findings on  $^{18}\text{F}$ -FDG PET/CT. We found a good sensitivity of 89.3% and specificity of 75.7% at a SUVmax cutoff value of 2.45 with an AUC of 0.907, which brought a better equilibrium between sensitivity and specificity.

Of 135 patients suspected of IM, 37 cases were eventually confirmed to be free of IM by PET/CT examination and follow-up. IM was overestimated in clinical practice.

There are 3 possible reasons for this: first, the clinical manifestations of IMs are non-specific, and similar clinical manifestations of other diseases lead to misdiagnosis; second, patients were referred to this institution from hospitals and clinics of different sizes, and the diagnostic level was different; third, clinicians over-rely on PET/CT and do not screen patients carefully before requesting PET/CT examination. PET/CT improved the diagnostic accuracy of IMs.

Our study has some limitations. The sample was from a single center and relatively small due to the rarity of LM; MRI images were predominantly from external hospitals, we just reviewed the reports, and detailed MRI data were not retrieved for analysis; the period over which data were collected was long and may have led to differences in the technique of MR imaging and PET imaging; breast cancer and melanoma are also common primary tumors of SLM, but they were not present in our sample. Multiple centers and large population studies will be the focus of further work in the future, which allows for an investigation of factors associated with SLM conspicuity on  $^{18}\text{F}$ -FDG PET/CT. The development of novel tracers is also promising in SLM diagnosis (10,11).

## Conclusions

We described  $^{18}\text{F}$ -FDG PET/CT imaging findings of SLM in 16 patients. Combined with the medical history, PET/CT has a good diagnostic yield in patients with SLM. A comparison of PET/CT with MRI for the diagnosis of SLM showed no significant difference in the sensitivity, specificity, or accuracy between the 2 imaging modalities. However, PET/CT revealed more and earlier nodular diseases, and MRI described it more accurately. ROC analysis revealed that the cutoff value of SUVmax 2.45 brought a better trade-off in sensitivity and specificity of SLM diagnosis.  $^{18}\text{F}$ -FDG PET/CT is an optional imaging modality to evaluate for suspected SLM and it should be performed early. There is a synergistic effect of whole-body  $^{18}\text{F}$ -FDG PET-CT scan to gadolinium-enhanced MRI.

## Acknowledgments

*Funding:* None.

## Footnote

*Reporting Checklist:* The authors have completed the STARD

reporting checklist. Available at <https://qims.amegroups.com/article/view/10.21037/qims-23-286/rc>

*Conflicts of Interest:* All authors have completed the ICMJE uniform disclosure form (available at <https://qims.amegroups.com/article/view/10.21037/qims-23-286/coif>). The authors have no conflicts of interest to declare.

*Ethical Statement:* The authors are accountable for all aspects of the work in ensuring that questions related to the accuracy or integrity of any part of the work are appropriately investigated and resolved. The study was conducted in accordance with the Declaration of Helsinki (as revised in 2013). The study was approved by the Institutional Ethics Committee of Jiangxi Provincial People's Hospital, and the requirement for individual consent for this retrospective analysis was waived.

*Open Access Statement:* This is an Open Access article distributed in accordance with the Creative Commons Attribution-NonCommercial-NoDerivs 4.0 International License (CC BY-NC-ND 4.0), which permits the non-commercial replication and distribution of the article with the strict proviso that no changes or edits are made and the original work is properly cited (including links to both the formal publication through the relevant DOI and the license). See: <https://creativecommons.org/licenses/by-nc-nd/4.0/>.

## References

1. Boire A. Metastasis to the Central Nervous System. *Continuum (Minneapolis)* 2020;26:1584-601.
2. Le Rhun E, Galanis E. Leptomeningeal metastases of solid cancer. *Curr Opin Neurol* 2016;29:797-805.
3. Hinke M, Skovran A, Dusini N, Azim S. Leptomeningeal Carcinomatosis: A Case Report and Literature Review. *Cureus* 2022;14:e26790.
4. Sener U, Kumthekar P, Boire A. Advances in the diagnosis, evaluation, and management of leptomeningeal disease. *Neurooncol Adv* 2021;3:v86-95.
5. Karam MB, Doroudinia A, Behzadi B, Mehrian P, Koma AY. Correlation of quantified metabolic activity in nonsmall cell lung cancer with tumor size and tumor pathological characteristics. *Medicine (Baltimore)* 2018;97:e11628.
6. Lu Y, Wang L, Ajani JA. Rare Esophageal Leptomeningeal Metastases Detected on  $^{18}\text{F}$ -FDG PET/CT. *Clin Nucl Med* 2020;45:334-5.

7. Erhamamcı S, Reyhan M, Altinkaya N. A case of brain and leptomeningeal metastases from urothelial carcinoma of the bladder. *Rev Esp Med Nucl Imagen Mol* 2014;33:290-2.
8. Grande ML, Rayo JI, Serrano J, Infante JR, Garcia L, Duran C, Gomez-Caminero F. Leptomeningeal carcinomatosis as only pathological finding at FDG-PET/CT in case of tumor marker elevation in breast cancer. *Indian J Nucl Med* 2014;29:53-4.
9. Shah S, Rangarajan V, Purandare N, Luthra K, Medhi S. 18F-FDG uptakes in leptomeningeal metastases from carcinoma of the breast on a positron emission tomography/computerized tomography study. *Indian J Cancer* 2007;44:115-8.
10. Lee Y, Yoo IR, Ha S. 18F-FES PET/CT for Characterization of Brain and Leptomeningeal Metastasis in Double Primary Cancer Patient. *Clin Nucl Med* 2022;47:e554-6.
11. Hao B, Wu J, Pang Y, Sun L, Chen H. 68Ga-FAPI PET/CT in Assessment of Leptomeningeal Metastases in a Patient With Lung Adenocarcinoma. *Clin Nucl Med* 2020;45:784-6.
12. Le Rhun E, Weller M, Brandsma D, Van den Bent M, de Azambuja E, Henriksson R, Boulanger T, Peters S, Watts C, Wick W, Wesseling P, Rudà R, Preusser M; . EANO-ESMO Clinical Practice Guidelines for diagnosis, treatment and follow-up of patients with leptomeningeal metastasis from solid tumours. *Ann Oncol* 2017;28:iv84-99.
13. Wang N, Bertalan MS, Brastianos PK. Leptomeningeal metastasis from systemic cancer: Review and update on management. *Cancer* 2018;124:21-35.
14. Le Rhun E, Taillibert S, Chamberlain MC. Carcinomatous meningitis: Leptomeningeal metastases in solid tumors. *Surg Neurol Int* 2013;4:S265-88.
15. Chuang TL, Chen JC, Chen YR, Wang YF. FDG PET/CT of Benign Psammomatous Meningioma Effacing the Medulla. *Clin Nucl Med* 2021;46:252-4.
16. Choudhury S, Purandare N, Shah S, Agrawal A, Rangarajan V. 18 F-FDG PET/CT Appearance of Radiation-Induced Delayed Transverse Myelitis. *Clin Nucl Med* 2022;47:e589-90.
17. Lopci E, Rodari M, Pepe G, Antunovic L, Chiti A. Imaging acute spinal myelitis with 18F-FDG PET/CT. *Eur J Nucl Med Mol Imaging* 2014;41:399-400.
18. Gao X, Pan R, Chen M, Zhao J, Zhong W, Wang H, Si X, Zhang X, Zhang L, Xu Y, Wang M. Leptomeningeal enhancement in magnetic resonance imaging predicts poor prognosis in lung adenocarcinoma patients with leptomeningeal metastasis. *Thorac Cancer* 2022;13:1059-66.
19. Bhatt G, Jain A, Bhatt A, Civelek AC. Intramedullary spinal cord metastases and whole body (18)F-FDG PET-CT-A case report. *Quant Imaging Med Surg* 2019;9:530-4.
20. Tan X, Li D, Wu X, Yang Y, Hou Q, He L, Jiang L. Physiologically intense FDG uptake of distal spinal cord on total-body PET/CT. *Ann Nucl Med* 2022;36:643-50.
21. Bhatt G, Li XF, Jain A, Sharma VR, Pan J, Rai A, Rai SN, Civelek AC. The normal variant (18)F FDG uptake in the lower thoracic spinal cord segments in cancer patients without CNS malignancy. *Am J Nucl Med Mol Imaging* 2013;3:317-25.

**Cite this article as:** Luo ZH, Lu PX, Qi WL, Jin AF, Liu Q, Zeng QY, Lu P. The sensitivity and specificity of <sup>18</sup>F-FDG PET/CT in spinal leptomeningeal metastases: the synergistic effect of the <sup>18</sup>F-FDG PET-CT to gadolinium-enhanced MRI. *Quant Imaging Med Surg* 2023;13(10):6863-6875. doi: 10.21037/qims-23-286